

Collective clusterization effects in light heavy ion reactions

Raj K. Gupta^a, M. Balasubramaniam^a, Rajesh Kumar^a, Dalip Singh^a, and C. Beck^b

^aPhysics Department, Panjab University, Chandigarh-160014, India

^bInstitut de Recherches Subatomiques, UMR7500, IN2P3/ Université Louis Pasteur, B.P. 28, F-67037 Strasbourg Cedex 2, France

The collective clusterization process, proposed for intermediate mass fragments (IMFs, $4 < A \leq 28$, $2 < Z \leq 14$) emitted from the hot and rotating compound nuclei formed in low energy reactions, is extended further to include also the emission of light particles (LPs, $A \leq 4$, $Z \leq 2$) from the fusion-evaporation residues. Both the LPs and IMFs are treated as the dynamical collective mass motion of preformed clusters through the barrier. Compared to IMFs, LPs are shown to have different characteristics, and the predictions of our, so-called, dynamical cluster-decay model are similar to those of the statistical fission model.

1. INTRODUCTION

For $A_{CN}^* \geq 48$, the compound nucleus (CN) so formed decays subsequently by the emission of mainly the LPs (n, p, α and γ -rays), and a significant (5-10%) decay strength is observed for the complex IMFs. The measured angular distributions and energy spectra for IMFs are consistent with fission-like decays of the respective CN.

The statistical Hauser Feshbach (HF) analysis, given for LPs emission, is also used to include the IMFs emission (BUSCO code [1], or the Extended HF scission-point model (EHFM) [2]). For IMFs, a more accepted process is the binary fission of the CN (fusion-fission), worked out in the statistical scission-point fission model [3] or the saddle-point "transition-state" model (TSM) [4,5], with the LPs still treated within the HF method.

The recently advanced dynamical cluster-decay model (DCM) [6] include the missing structure information of the statistical fission models, by taking each fragment (LP or IMF) preformed in the CN, which subsequently follows the dynamical cluster-decay process rather than the fission process of the statistical model. The structure information influences the observed yields strongly through the observed strong resonance behaviour in the measured excitation functions of large-angle elastic and inelastic scattering yields (see, e.g., [7]), which enters the DCM via the preformation probability of the fragments.

The DCM for hot and rotating compound systems is a reformulation of the preformed cluster model (PCM) of Gupta et al. [8,9] for ground-state decays, briefly developed in Section 2. The application of DCM to $^{32}\text{S} + ^{24}\text{Mg} \rightarrow ^{56}\text{Ni}^*$ is discussed in section 3. The $^{56}\text{Ni}^*$ has a negative Q-value (Q_{out}), with experimental mass distributions of both LPs and IMFs being available [4]. The model has also been applied successfully for the positive Q-value $^{116}\text{Ba}^*$ system. A summary of our results is presented in section 4.

2. THE DCM FOR HOT AND ROTATING NUCLEI

The DCM uses collective coordinates of mass (charge) asymmetry $\eta=(A_1-A_2)/(A_1+A_2)$ ($\eta_Z=(Z_1-Z_2)/(Z_1+Z_2)$), and relative separation R , characterizing, respectively, the nucleon-exchange between the outgoing fragments, and the incident channel kinetic energy (E_{cm}) transferred to internal excitation of outgoing channel ($E_{CN}^*+Q_{out}(T)=TKE(T)+TXE(T)$; TXE and TKE as the total excitation and kinetic energy), since $R \equiv R(T, \eta)$. For decoupled R -, η -motions, in terms of partial waves, the fragment formation or CN decay cross-section

$$\sigma = \frac{\pi}{k^2} \sum_{l=0}^{l_c} (2l+1) P_0 P; \quad k = \sqrt{\frac{2\mu E_{cm}}{\hbar^2}}. \quad (1)$$

The preformation probability P_0 , referring to η -motion, is the solution of stationary Schrödinger eqn. in η (with T -dependent collective fragmentation potentials [10,11,12]), at a fixed

$$R = R_a = C_t(\eta, T) + \overline{\Delta R}(T). \quad (2)$$

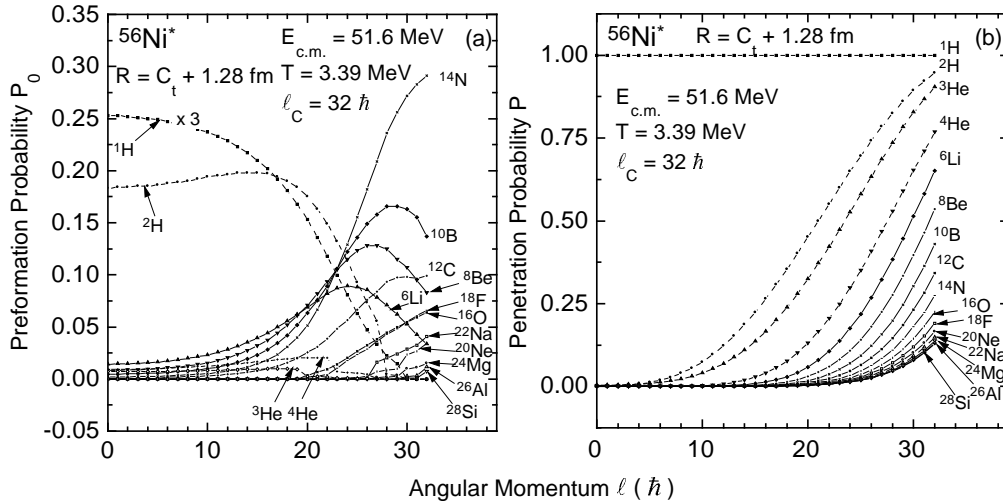


Figure 1. (a) $P_0(\ell)$ (b) $P(\ell)$ for decay of $^{56}\text{Ni}^*$ at $T=3.39$ MeV.

C_i are Süssmann radii and T is from $E_{CN}^* = E_{cm} + Q_{in} = (A/9)T^2 - T$. $\overline{\Delta R}(T)$, the only parameter of model, simulating the two-centre nuclear shape, is similar to neck-length used in statistical models [2,5]. The penetrability P , referring to R -motion, is the WKB integral, with $V(R_a) = V(R_b) = Q_{eff}$. R_b is second turning point. Q_{eff} , the effective Q -value or $TKE(T, \ell=0)$, is $Q_{eff}(T) = B(T) - [B_1(T=0) + B_2(T=0)] = TKE(T) = V(R_a)$, for the CN at T to decay to two observed cold fragments ($T=0$). This transition occurs by emitting LPs of energy $E_x = B(T) - B(0) = Q_{eff}(T) - Q_{out}(T=0)$. Instead, here we use Eq. (2). $\ell_c = R_a \sqrt{2\mu[E_{cm} - V(R_a, \eta_{in}, \ell=0)]}/\hbar$, with μ and R_a referring to entrance channel η_{in} .

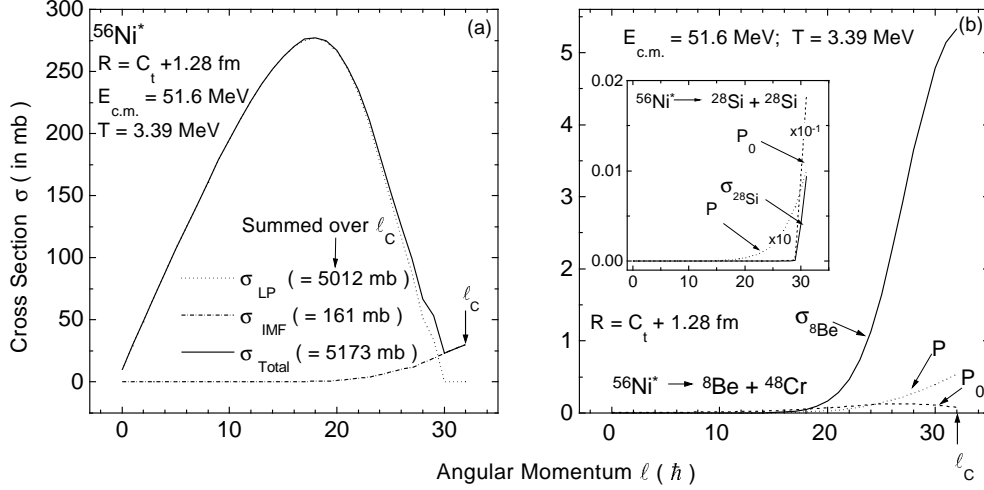


Figure 2. The calculated (a) $\sigma_{LP}(\ell)$, $\sigma_{IMF}(\ell)$ and their sum $\sigma_{Total}(\ell)$; (b) $P_0(\ell)$, $P(\ell)$ and $\sigma_{IMF}(\ell)$ for ${}^8\text{Be}$ and ${}^{28}\text{Si}$ decays of ${}^{56}\text{Ni}^*$ at $T=3.39$ MeV.

3. CALCULATIONS

Fig. 1 gives the variation of P_0 and P with ℓ for both the LPs ($A \leq 4$) and IMFs ($A > 4$) referring to energetically favoured fragments. Interestingly, the behaviour of LPs is different from that of the IMFs; whereas for LPs P_0 decreases with increase of ℓ , for IMFs it increases as ℓ increases and then starts to decrease at a large ℓ -value. Thus, LPs contribute to P_0 for smaller ℓ -values whereas the same for IMFs is important for higher ℓ 's ($> 18\hbar$). Similarly, the P 's for LPs are large at all ℓ -values, whereas the same for $\ell \leq 18\hbar$ is nearly zero for all IMFs. This means that the lower ℓ 's contribute only towards LPs cross-section σ_{LP} and the higher ℓ 's ($> 18\hbar$) to fission-like, IMFs cross-section σ_{IMF} , as shown in Fig. 2(a). The total cross-section $\sigma_{Total} = \sigma_{LP} + \sigma_{IMF}$ is also plotted, and the summed up cross-sections are given in braces, to be compared with experiments.

Fig. 2(b) illustrates the contributions of individual IMFs. Apparently, the lighter IMFs contribute more than the heavier IMFs towards σ_{IMF} , pointing to the observed favourable asymmetric mass distribution. Interestingly, similar results, as presented by Figs. 2(a) and 2(b), are obtained by the statistical fission model [2,4] (see e.g. Fig. 14 in [4]).

Fig. 3(a) shows the summed up σ for decay of ${}^{56}\text{Ni}^*$ at $E_{c.m.} = 51.6$ MeV to both the LPs and even-A, $N=Z$ IMFs, along with the TSM and EHFM calculations, compared with the experimental data [4]. The TSM and EHFM for LPs are the HF results, whereas the DCM treats both the LPs and IMFs emissions on similar footings. For the LPs emission, the measured $\sigma_{LP} = 1050 \pm 100$ mb but the separate yield for each emitted light particle is not available for a direct comparison. First of all, we notice in Fig. 3(a) that the unphysical discontinuity at the point between $A_2 = 4$ and 6 in TSM is not present in our DCM results. In DCM, σ_{LP} is over-estimated by a large factor of ~ 5 , a discrepancy that gets removed if mass-one-particle (proton) is replaced with neutron, for example. This signifies the importance of the contributing particles to σ_{LP} . For the IMFs, the general comparison between the data and DCM is of similar quality as for the TSM or EHFM

model, at least for $A_2 \leq 22$. The use of Q_{eff} improves the comparison slightly.

Fig. 3(b) shows the average $\overline{TKE} = \sum_{\ell=0}^{\ell_c} \sigma_{\ell}(TKE)_{\ell} / \sigma$, with $\sigma = \sum \sigma_{\ell}$, compared with experimental data [4]. Apparently, the comparisons are reasonably good. The maximum ℓ -value is less than ℓ_c -value, which may be due to the use of $\overline{\Delta R}$ instead of actual $\Delta R(\eta)$.

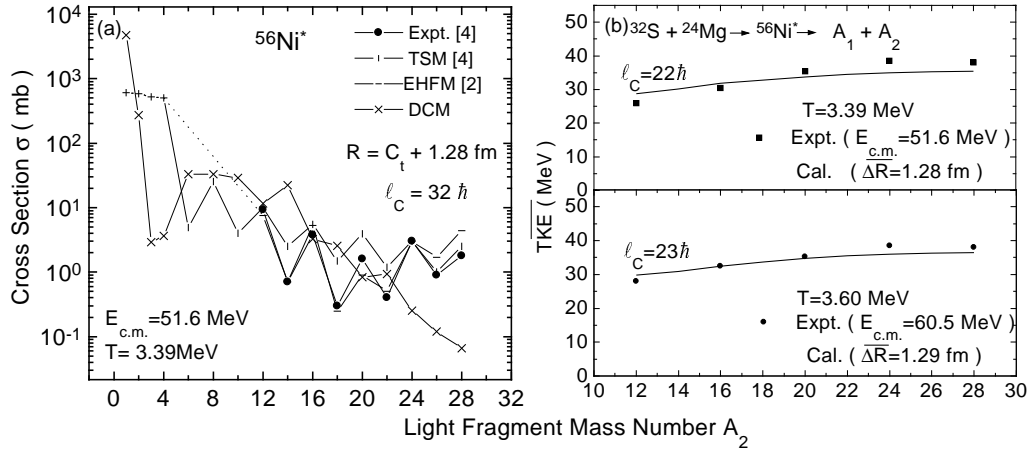


Figure 3. (a) The calculated $\sigma(A_2)$ on DCM, EHF [2] and TSM [4], compared with experimental data [4]; (b) The measured and calculated \overline{TKE} at $E_{c.m.} = 51.6, 60.5$ MeV.

4. CONCLUSIONS

The dynamical collective clusterization is shown as an alternative good decay process for both the LPs and IMFs produced in low energy reactions. The IMFs are shown to be produced as clusters, like in cluster radioactivity, but from excited CN. The LPs are also considered to be of the same origin, without invoking any statistical evaporation process.

REFERENCES

1. J. Gomez del Campo, et al., Phys. Rev. C43 (1991) 2689.
2. T. Matsuse, et al., Phys. Rev. C55 (1997) 1380.
3. R.J. Charity, et al., Nucl. Phys. A483 (1988) 43.
4. S.J. Sanders, et al., Phys. Rev. C40 (1989) 2091.
5. S.J. Sanders, Phys. Rev. C44 (1991) 2676.
6. R.K. Gupta et al., Phys. Rev. C65 (2002) 024601, C68 (2003) 014610; Heavy Ion Phys. 18 (2003) Nos. 2-4, J. Phys. G: Nucl. Part. Phys. 29 (2003) 2703.
7. C. Beck, et al., Phys. Rev. C63 (2001) 014607.
8. S.S. Malik and R.K. Gupta, Phys. Rev. C39 (1989) 1992.
9. S. Kumar and R.K. Gupta, Phys. Rev. C49 (1994) 1922.
10. N.J. Davidson, et al., Nucl. Phys. A570 (1994) 61c.
11. W. Myers and W.J. Swiatecki, Nucl. Phys. 81 (1966) 1.
12. G. Royer, J. Phys. G: Nucl. Part. Phys. 18 (1992) 1781.